Nature and evolution of the band-edge states in MoS_{2}: From monolayer to bulk

J. E. Padilha, H. Peelaers, A. Janotti, and C. G. Van de Walle

Phys. Rev. B **90**, 205420 — Published 17 November 2014

DOI: 10.1103/PhysRevB.90.205420

Nature and evolution of the band-edge states in MoS_2: from monolayer to bulk

J. E. Padilha,[1,2,*] H. Peelaers,[2] A. Janotti,[2] and C. G. Van de Walle[2,†]

[1] *Instituto de Física, Universidade de São Paulo, CP 66318, 05315-970, São Paulo, SP, Brazil.*

[2] *Materials Department, University of California, Santa Barbara, California 93106-5050, USA*

Abstract

Exploring two-dimensional layered materials, such as molybdenum disulfide (MoS_2), for (opto)electronic applications requires detailed knowledge of their electronic band structure. Using first-principles calculations we trace the evolution of the band structure as a function of the number of layers, starting from a monolayer, which has a direct gap, to the bulk material, which has an indirect gap. We find that, with respect to the vacuum level, the valence-band maximum (VBM) increases rapidly with the number of layers, while the conduction-band minimum (CBM) remains almost constant. For two or more layers the VBM always occurs at Γ and the CBM occurs at K. These findings are analyzed in terms of the orbital composition of the valence- and conduction-band edges at the various high-symmetry points in the Brillouin zone.

PACS numbers: 71.20.Nr, 71.80.Ga,73.22.-f

Two-dimensional (2D) materials have become an important subject of research over the past few years after the isolation of 2D graphene.[1–3] The electronic band structure of graphene features a cone-shaped linear dispersion, the Dirac cone, near the Fermi level, with important implications for nanoelectronics.[4,5] Despite its exquisite electronic properties and the rapid advances in graphene research, a major drawback for applications in electronics is the absence of a band gap. This has spawned a search for other 2D layered materials that do exhibit band gaps.[6]

The 2D transition-metal dichalcogenides (MX_2, where M=Mo, W,..., and X=S, Se, or Te) have band gaps in the range of 1–2 eV and are considered strong candidates for nanoelectronic and optoelectronic devices.[7–11] MoS_2 has a direct band gap of 1.9 eV in a monolayer[12] and an indirect band gap of 1.3 eV in the bulk.[13] Prototype transistors with electron mobility as high as $\sim$500 $cm^2V^{-1}s^{-1}$ and high on/off ratio of $\sim 10^8$ have been demonstrated.[7,14] Studies to date have mainly focused on monolayer, bilayer and bulk MoS_2. They all agree that monolayer MoS_2 exhibits a direct band gap at the K point. For the bilayer the reports disagree. Some studies find an indirect gap from Γ to K,[15–18] while others suggest that the gap is indirect from Γ to $\Lambda_{\rm min}$[19–21] [$\Lambda_{\rm min}$ indicates the location of the conduction-band minimum (CBM) and is located on the Γ-K line, indicated in Fig. 1(b)]. For bulk most studies find an indirect gap from Γ to $\Lambda_{\rm min}$. There is also no consensus on how the band structure evolves going from a monolayer to the bulk. Resolving these disagreements is key to applications of MoS_2 in (opto)electronics.

We address these issues by performing first-principles calculations for the electronic structure of MoS_2 as a function of the number of layers (n=1,..,7) up to the bulk limit. Van der Waals interactions are included, which is important for obtaining the correct atomic structure, which is strongly coupled to the electronic structure. Spin-orbit coupling (SOC) is also included, as this influences the splitting of the band edges. We will discuss our results in terms of the orbital composition of the band-edge states at the various high-symmetry points of the Brillouin zone, thereby providing new insights into the electronic structure of MoS_2.

Our calculations are based on density functional theory (DFT),[22,23] as implemented in the VASP code.[24] Standard functionals underestimate the band gap. Therefore we utilize the hybrid functional of Heyd, Scuseria, and Ernzerhof (HSE06),[25,26] which gives more accurate band gaps and at the same time also accurate structural properties. We use projector

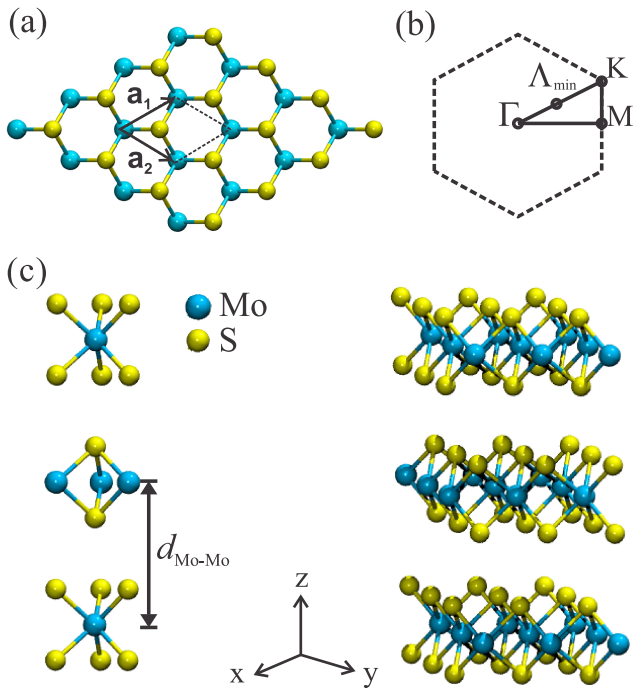

FIG. 1. (Color online)(a) Top view of a monolayer of MoS_2. The lattice vectors ($\mathbf{a}_1$ and $\mathbf{a}_2$) that define the unit cell are indicated by vectors, and the outline of the unit cell by dashed lines. (b) The Brillouin zone, with the relevant high-symmetry k-points indicated. (c) The structure of trilayer 2H-MoS_2. In the 2H stacking the S atoms in each layer are located directly above/below the Mo atom in the neighboring layer.

augmented wave (PAW) potentials[27] and a plane-wave basis set with a 350 eV energy cutoff. MoS_2 with a finite number of layers (n=1,..,7) is simulated using a slab geometry with 17 Å of vacuum, to avoid spurious interactions with the periodic images. The Brillouin zone is sampled with a 9×9×1 k-point sampling, increased to 9×9×6 for the bulk system. Excitonic effects are not explicitly included, so the reported band gaps are the fundamental band gaps. The van der Waals interactions are included by using the semi-empirical D2 method.[28] This method reproduces the experimental interlayer distance.[29] The valence-band (VB) and conduction-band (CB) edges with respect to the vacuum level are determined by aligning the planar-averaged electrostatic potential within the layer with the vacuum region. A major advantage of our HSE06-D2 methodology over calculations with the GW method[15,17,30–34] is that our approach is more consistent: it includes van der Waals interactions and SOC and is internally consistent because of the capability to evaluate both atomic and electronic structure. The GW approach, on the other hand, relies on the experimental structure, or

on structures obtained with a lower-level method.

Lattice parameters and atomic positions for all structures are relaxed until residual forces on the atoms are smaller than 0.001 eV/Å. For the in-plane equilibrium lattice parameters [the length of the vectors $\mathbf{a_1}$ and $\mathbf{a_2}$, indicated in Figure 1(a)] we obtain a=3.16 Å, and for the interlayer distance $d_{\mathrm{Mo-Mo}}$=6.19 Å, shown in Figure 1(c). Both are in good agreement with experiment (a=3.16 Å and $d_{\mathrm{Mo-Mo}}=c/2$=6.15 Å[35]). We find that a and $d_{\mathrm{Mo-Mo}}$ are virtually independent of the number of layers, varying by less than 5×10^{-3} Å.

The calculated electronic band structures for n=1,2, and 3 layers, and for bulk are shown in Figure 2, both with and without SOC. The high-symmetry points are schematically indicated in the Brillouin zone drawn in Figure 1(b). The monolayer exhibits a direct band gap of 2.06 eV, located at the K point. The valence-band maximum (VBM) at K is 158 meV higher in energy than the local maximum at Γ. For the bilayer, trilayer, and bulk the band gap is indirect, with the VBM occurring at Γ and the conduction-band minimum at K. This agrees with recent experimental measurements[36] of the valence bands. We also find that while the minimum at the Λ_{min} point decreases in energy with the number of layers, it always remains higher than the CBM at K; for bulk MoS_2, it is 24 meV higher in energy than the CBM at K. These results agree with the reports in Refs.,[15–18,37] which assign an indirect gap at Γ-K to the bilayer, but disagree with Refs.,[19–21] which report a minimum band gap at Γ-Λ_{min}. These differences can be attributed, in part, to strain.

It was shown that for tensile biaxial strain in bilayers the CBM is located at K, while for sufficiently large compressive strain, the CBM is at Λ_{min}.[38]Strain has a similar effect in trilayer[39] and bulk[40] MoS_2. For bulk all reported studies agree that the CBM is at the Λ_{min}.[17–19,21,31,32,37,40,41] In our calculations we find the CBM at K, but the difference between the K and Λ_{min} edge is very small (24 meV). Note that having an accurate value for the out-of-plane lattice parameter, which requires taking into account vdW interactions, is important for correctly describing the electronic structure of MoS_2. Without vdW interactions, PBE and HSE06 significantly overestimate the out-of-plane lattice parameter,[29] raising the conduction-band edge at Λ_{min}, thus placing the CBM at the K point.[20,40] This large dependency of the band structure on the in-plane and out-of-plane lattice constants illustrates the importance of having an accurate and consistent methodology.

Inclusion of SOC [Fig. 2(e-h)] mainly leads to a splitting of the valence band at K and of the conduction band at Λ_{min}. It does not affect the location of the VBM or CBM, and

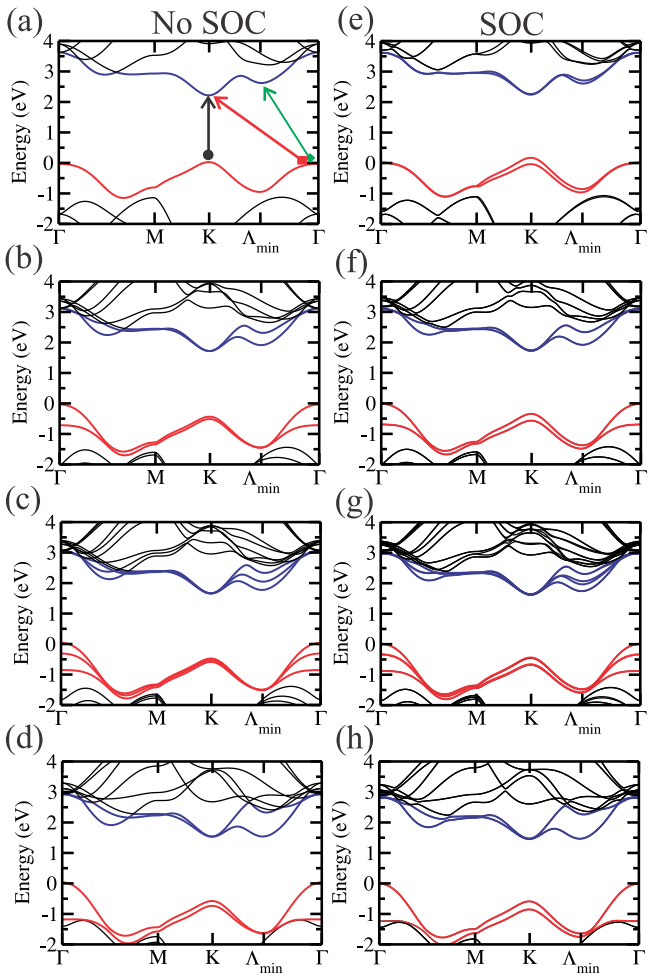

FIG. 2. (Color Online) Evolution of the band structure for (a) 1 layer, (b) 2 layers, (c) 3 layers, and (d) bulk MoS_2, without the inclusion of the SOC, and for (e) 1 layer, (f) 2 layers, (g) 3 layers, and (h) bulk MoS_2 including SOC. The highest valence band is shown in red and the lowest conduction band in blue. The arrows in (a) indicate the important band gaps (K-K—black circle arrow; Γ-K—square red arrow; Γ-$\Lambda_{\rm min}$—green diamond arrow;). The VBM is set to zero.

the absolute band gap shifts are smaller than 19 meV, except for the monolayer, where it reduces the band gap by 120 meV.

In Figure 3(a) we show the variation of the band gaps for n=1 to 7. All the band gaps decrease monotonically with increasing number of layers, and they converge rapidly to the bulk value. The K-K gap for n=5 is only 10 meV higher than in bulk, and it is equal to the bulk value for n=7. For Γ-K the difference with bulk is 70 meV for n=5 and 44 meV for n=7. This variation of the band gap has important consequences for the valley degeneracy. For the CB the degeneracy is 2 for monolayer, and with increasing number of layers, the CB

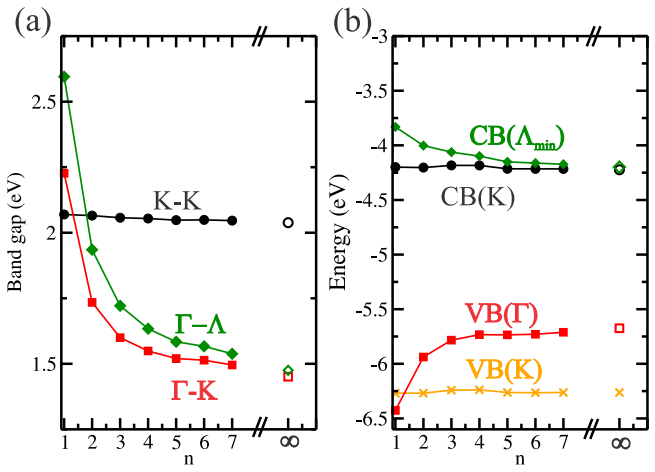

FIG. 3. (Color Online) (a) Evolution of the band gaps as a function of the number of layers (n). The black circles (K-K), red squares (Γ-K) and green diamonds (Γ-Λ_{min}) indicate the magnitude of the different band gaps. Hollow symbols indicate the bulk band gaps. (b) Position of the band edge with respect to the vacuum level for the VB at K (orange crosses), VB at Γ (red squares), CB at K (black circles), and CB at Λ_{min} (green diamonds).

edge at Λ_{min} also becomes important, leading to an additional valley degeneracy of 6. For the VB the degeneracy is 2 for monolayer and 1 for all other layers.

It is highly informative to inspect the band edges on an absolute energy scale, i.e., with respect to the vacuum level. Such an analysis provides insight into the physical origins of the band-gap variations; in addition, it helps in screening materials for ohmic and Schottky contacts[42] and determines band alignments in heterostructures.[43] The evolution as a function of the number of layers n is shown in Figure 3(b), showing that both the VB and CB edges at K exhibit only small variations (smaller than 50 meV). The reason for this behavior is elucidated by inspecting the character of the orbitals that form the band-edge states, as shown in Figure 4. The axes are aligned as shown in Figure 1(c), where x and y are in-plane and z is out-of-plane. The VB edge at K is composed of S p_x and p_y orbitals, and Mo d_{xy} and $d_{x^2-y^2}$ orbitals. These are all oriented along the in-plane direction and are therefore only slightly perturbed when additional layers of MoS_2 are added. This explains the appearance of the almost degenerate bands at the VB edge at the K point, with each layer contributing one band. The CB edge at K is composed mainly of S p_x and p_y orbitals and Mo d_{z^2} orbitals. When additional layers are added, the bands that form the CBM at K do not couple by symmetry, explaining the n-fold degeneracy of the CBM at K, where n is the number of

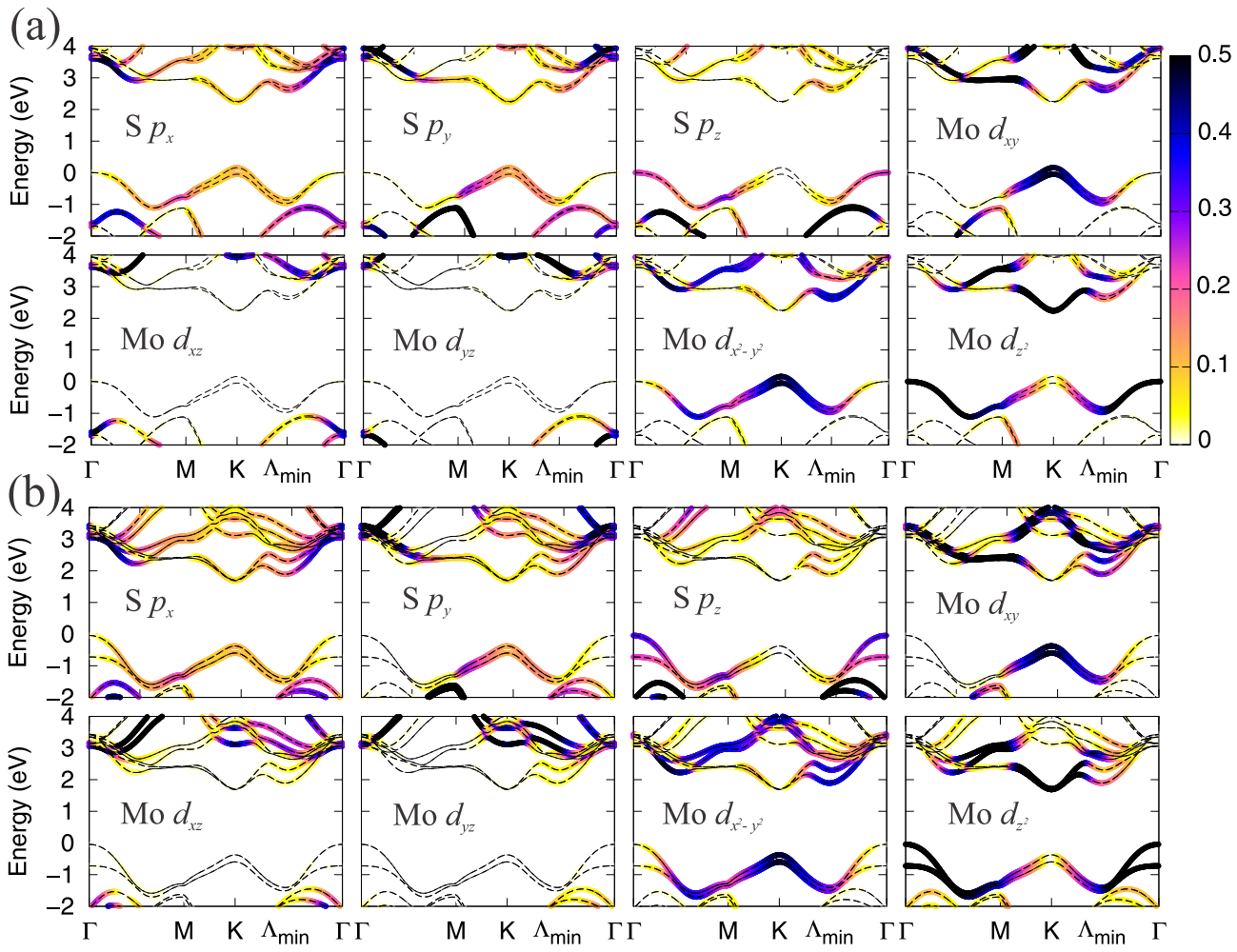

FIG. 4. (Color Online) Orbital-projected band structure for (a) monolayer MoS_2 and (b) bilayer MoS_2. The projections are made on the S p orbitals and the Mo d orbitals. The scale indicates the magnitude of the projection. The dashed lines indicate the band structure.

layers. The absolute position of the VBM for a monolayer agrees well with a previously reported value, obtained with the PBE0 hybrid functional.[44] Our VB edge position for 6 layers is 0.51 eV lower than reported in Ref. 41 based on PBEsol and G_0W_0. However, it has been noted[30,31] that the absolute position of the VBM in GW calculations is very sensitive to the convergence parameters.

The results shown in Figure 4 also explain the transition from a direct band gap for the MoS_2 monolayer to an indirect band gap for $n > 1$. As shown in Figure 4(a), the VB at Γ is composed of out-of-plane p_z S and d_{z^2} Mo orbitals. Each layer again contributes one band, and because of the nature of these orbitals the bands at Γ interact strongly. When the

number of layers is increased, the degeneracy is lifted and a splitting of the bands occurs, which pushes the VBM to higher energy. This allows us to understand the evolution shown in Figure 3. The variation of the band gap is largely driven by the variation of the VB at Γ. Going from a monolayer to a bilayer significantly raises the VB at Γ, resulting in a transition from the direct K-K gap to an indirect Γ-K gap. As more layers are stacked, the VBM at Γ increases monotonically, coming within 44 meV of the bulk value for $n = 7$.

The evolution of the VB states at Γ as a function of n is clearly crucial for the electronic structure, and we examine it in more detail in Figure 5. For the monolayer there is only one nondegenerate state at Γ, composed of S p_z and Mo d_{z^2} [Figure 4(a)]. The corresponding wavefunction Ψ_1 is shown in Figure 5(b); since it is a wavefunction at Γ, it is purely real. For n=2, the highest VB splits into two states, Ψ_{2b} and Ψ_{2a} [Figure 5(a))]. The bonding and antibonding character of these states is evident in Figure 5(b), and Figure 4(b) shows that these states are composed from combinations of S p_z and Mo d_{z^2} orbitals. It is the antibonding state that forms the VBM. For three or more layers we see that the lowest energy state always consists of a fully symmetric combination of Mo d_{z^2} and S p_z in each of the constituting layers [e.g., Ψ_{3c} in Figure 5(b)]. The orbital-projected band structure is very similar to the one shown in Figure 4(b), and since little or no additional information is conveyed, it is not shown here. The higher-lying states are the orthogonal antisymmetric combinations. The gap is governed by the position of the highest energy state, which is an antisymmetric state. This state converges quickly to the bulk value when the number of layers is increased, as was shown before. This splitting of the VB states was also observed experimentally.[36]

Finally, we discuss the CB edge at $\Lambda_{\min}$, which has contributions from all S p orbitals (p_x, p_y, and a lesser amount of p_z) and of Mo d_{xy}, $d_{x^2-y^2}$, and d_{z^2}. Splittings similar to those at the Γ point therefore occur when layers are added, explaining why the CB edge at $\Lambda_{\min}$ exhibits the strong variation with number of layers seen in Figure 3(b).

We note that the orbital composition of the CB states at the K, Γ, and $\Lambda_{\min}$ points can also explain the changes in the type of band gap as a function of strain.[40] Orbitals that extend out of the plane, i.e., the S p_z orbitals, are sensitive to changes in the interlayer distance, while in-plane orbitals, such as S p_x and p_y, and Mo d_{xy} and $d_{x^2-y^2}$, are more sensitive to in-plane strain. This emphasizes again the importance of correctly describing both the interlayer distance (and thus the need for including van der Waals interactions)

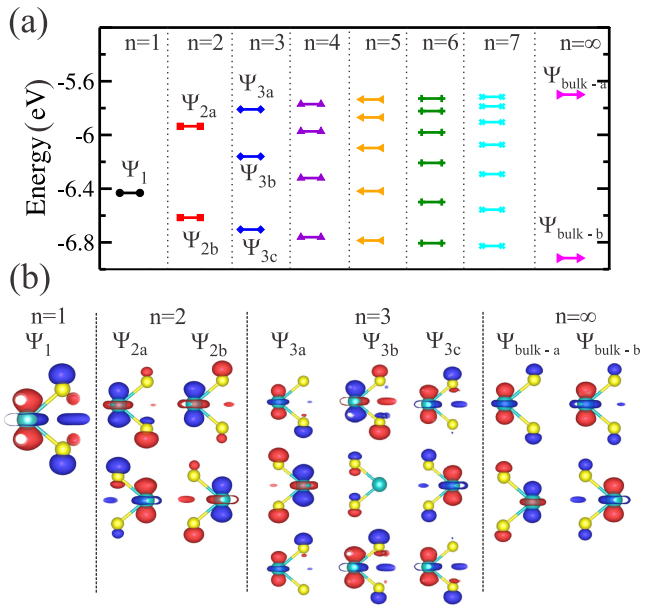

FIG. 5. (Color Online)(a) Energies of the highest VBs at the Γ point as a function of the number of layers, plotted with respect to the vacuum level. (b) Wavefunctions at Γ corresponding to the states labeled in (a), obtained using the OpenMX code.[45] Red (darker) indicates negative values, blue (lighter) positive values.

and in-plane lattice parameters (to avoid spurious strain).

In conclusion, we addressed the evolution of the band gap and band-edge states in MoS_2 as a function of the number of layers. The band structures were analyzed in terms of the orbital composition at the various high-symmetry points in the Brillouin zone. Among the band extrema, the valence-band maximum at Γ is the most sensitive to the interaction with adjacent layers, a feature we explained based on the character of the atomic orbitals. Our results elucidate the change from a direct band gap at the K point in the monolayer to an indirect Γ-K gap in the bilayer and multilayers.

I. ACKNOWLEDGEMENT

We are grateful to D. Jena for suggestions and discussions. This work was supported by the Brazilian agency FAPESP, by the Office of Science of the U.S. Department of Energy (Grant No. DE-FG02-07ER46434), by the Center for Low Energy Systems Technology (LEAST), one of the six SRC STARnet Centers sponsored by MARCO and DARPA, and

by the IMI Program of the National Science Foundation under Award No. DMR 08-43934. Computational resources were provided by the Extreme Science and Engineering Discovery Environment (XSEDE), supported by NSF (ACI-1053575 and DMR07-0072N).

---

* padilha@if.usp.br

† vandewalle@mrl.ucsb.edu

[1] K. S. Novoselov, A. K. Geim, S. V. Morozov, D. Jiang, Y. Zhang, S. V. Dubonos, I. V. Grigorieva, and A. A. Firsov, Science **306**, 666 (2004).

[2] K. S. Novoselov, A. K. Geim, S. V. Morozov, D. Jiang, M. I. Katsnelson, I. V. Grigorieva, S. V. Dubonos, and A. A. Firsov, Nature **438**, 197 (2005).

[3] A. K. Geim and K. S. Novoselov, Nat. Mater. **6**, 183 (2007).

[4] F. Schwierz, Nat. Nanotechnol. **5**, 487 (2010).

[5] Y.-M. Lin, C. Dimitrakopoulos, K. A. Jenkins, D. B. Farmer, H.-Y. Chiu, A. Grill, and P. Avouris, Science **327**, 662 (2010).

[6] S. Z. Butler, S. M. Hollen, L. Cao, Y. Cui, J. A. Gupta, H. R. Gutie, T. F. Heinz, S. S. Hong, J. Huang, A. F. Ismach, E. Johnston-Halperin, M. Kuno, V. V. Plashnitsa, R. D. Robinson, R. S. Ruoff, S. Salahuddin, J. Shan, L. Shi, O. M. G. Spencer, M. Terrones, W. Windl, and J. E. Goldberger, ACS Nano **7**, 2898 (2013).

[7] W. Bao, X. Cai, D. Kim, K. Sridhara, and M. S. Fuhrer, Appl. Phys. Lett. **102**, 042104 (2013).

[8] M. Bernardi, M. Palummo, and J. C. Grossman, Nano Lett. **13**, 3664 (2013).

[9] D. Lembke and A. Kis, ACS Nano **6**, 10070 (2012).

[10] H.-Y. Chang, S. Yang, J. Lee, L. Tao, W.-S. Hwang, D. Jena, N. Lu, and D. Akinwande, ACS Nano **7**, 5446 (2013).

[11] H. Liu, A. T. Neal, and P. D. Ye, ACS Nano **6**, 8563 (2012).

[12] K. F. Mak, C. Lee, J. Hone, J. Shan, and T. F. Heinz, Phys. Rev. Lett. **105**, 136805 (2010).

[13] A. R. Beal and H. P. Hughes, J Phys C Solid State **12**, 881 (1979).

[14] S. Kim, A. Konar, W.-S. Hwang, J. H. Lee, J. Lee, J. Yang, C. Jung, H. Kim, J.-B. Yoo, J.-Y. Choi, Y. W. Jin, S. Y. Lee, D. Jena, W. Choi, and K. Kim, Nat. Commun. **3**, 1011 (2012).

[15] J. He, K. Hummer, and C. Franchini, Phys. Rev. B **89**, 075409 (2014).

[16] W. Zhao, R. M. Ribeiro, M. Toh, A. Carvalho, C. Kloc, A. H. Castro Neto, and G. Eda, Nano Lett. **13**, 5627 (2013).

[17] T. Cheiwchanchamnangij and W. R. L. Lambrecht, Phys. Rev. B **85**, 205302 (2012).

[18] W. S. Yun, S. W. Han, S. C. Hong, I. G. Kim, and J. D. Lee, Phys. Rev. B **85**, 033305 (2012).

[19] J. K. Ellis, M. J. Lucero, and G. E. Scuseria, Appl. Phys. Lett. **99**, 261908 (2011).

[20] A. Ramasubramaniam, D. Naveh, and E. Towe, Phys. Rev. B **84**, 205325 (2011).

[21] A. Kuc, N. Zibouche, and T. Heine, Phys. Rev. B **83**, 245213 (2011).

[22] P. Hohenberg and W. Kohn, Phys. Rev. **136**, B864 (1964).

[23] W. Kohn and L. J. Sham, Phys. Rev. **140**, A1133 (1965).

[24] G. Kresse and J. Furthmüller, Phys. Rev. B **54**, 11169 (1996).

[25] J. Heyd, G. E. Scuseria, and M. Ernzerhof, J. Chem. Phys. **118**, 8207 (2003).

[26] J. Heyd, G. E. Scuseria, and M. Ernzerhof, J. Chem. Phys. **124**, 219906 (2006).

[27] P. E. Blöchl, Phys. Rev. B **50**, 17953 (1994).

[28] S. Grimme, J. Comput. Chem. **27**, 1787 (2006).

[29] H. Peelaers and C. G. Van de Walle, J. Phys.: Condens. Matter **26**, 305502 (2014).

[30] F. Hüser, T. Olsen, and K. S. Thygesen, Phys. Rev. B **88**, 245309 (2013).

[31] H.-P. Komsa and A. V. Krasheninnikov, Phys. Rev. B **86**, 241201 (2012).

[32] A. Molina-Sánchez, D. Sangalli, K. Hummer, A. Marini, and L. Wirtz, Phys. Rev. B **88**, 045412 (2013).

[33] D. Y. Qiu, F. H. da Jornada, and S. G. Louie, Phys. Rev. Lett. **111**, 216805 (2013).

[34] A. Ramasubramaniam, Phys. Rev. B **86**, 115409 (2012).

[35] N. Wakabayashi, H. Smith, and R. Nicklow, Phys. Rev. B **12**, 659 (1975).

[36] W. Jin, P.-C. Yeh, N. Zaki, D. Zhang, J. T. Sadowski, A. Al-Mahboob, A. M. van der Zande, D. A. Chenet, J. I. Dadap, I. P. Herman, P. Sutter, J. Hone, and R. M. Osgood, Phys. Rev. Lett. **111**, 106801 (2013).

[37] S. Tongay, J. Zhou, C. Ataca, K. Lo, T. S. Matthews, J. Li, J. C. Grossman, and J. Wu, Nano Lett. **12**, 5576 (2012).

[38] E. Scalise, M. Houssa, G. Pourtois, V. Afanas'ev, and A. Stesmans, Nano Research **5**, 43 (2011).

[39] Y. Y. Hui, X. Liu, W. Jie, N. Y. Chan, J. Hao, Y.-T. Hsu, L.-J. Li, W. Guo, and S. P. Lau, ACS Nano **7**, 7126 (2013).

[40] H. Peelaers and C. G. Van de Walle, Phys. Rev. B. **86**, 241401 (2012).

[41] H. Jiang, J. Phys. Chem. C **116**, 7664 (2012).

[42] I. Popov, G. Seifert, and D. Tománek, Phys. Rev. Lett. **108**, 156802 (2012).

[43] A. K. Geim and I. V. Grigorieva, Nature **499**, 419 (2013).

[44] J. Kang, S. Tongay, J. Zhou, J. Li, and J. Wu, Appl. Phys. Lett. **102**, 012111 (2013).

[45] T. Ozaki, Phys. Rev. B **67**, 155108 (2003).